



LAWRENCE
LIVERMORE
NATIONAL
LABORATORY

LLNL-CONF-703005

Carbon Particles Produced by Detonation Waves

A. L. Kuhl

September 14, 2016

Multiphase Physics Deep Dive
St Petersburg, FL, United States
October 6, 2016 through October 7, 2016

Disclaimer

This document was prepared as an account of work sponsored by an agency of the United States government. Neither the United States government nor Lawrence Livermore National Security, LLC, nor any of their employees makes any warranty, expressed or implied, or assumes any legal liability or responsibility for the accuracy, completeness, or usefulness of any information, apparatus, product, or process disclosed, or represents that its use would not infringe privately owned rights. Reference herein to any specific commercial product, process, or service by trade name, trademark, manufacturer, or otherwise does not necessarily constitute or imply its endorsement, recommendation, or favoring by the United States government or Lawrence Livermore National Security, LLC. The views and opinions of authors expressed herein do not necessarily state or reflect those of the United States government or Lawrence Livermore National Security, LLC, and shall not be used for advertising or product endorsement purposes.

Carbon Particles Produced by Detonation Waves

Allen L. Kuhl

Lawrence Livermore National Laboratory
Livermore, California USA 94551

ABSTRACT

In this paper we review the topic of carbon particles produced by detonation waves. We summarize the thermodynamic equilibrium solutions, SEM photographs of carbon agglomerates, similarity solutions of the conductivity profiles in detonation waves, correlation of peak conductivity with carbon content of the explosive, and describe carbon agglomeration kinetics. Better knowledge of the agglomeration physics is needed to model optical and electromagnetic radiation from CHNO-based explosives.

INTRODUCTION

It has been recognized for more than 60 years, that detonation products gases can be conductive. In Cook's book: *The Science of High Explosives* [1] published in 1958, he devoted the entire Chapter 7 to the subjects of ionization, electrical, magnetic and electromagnetic phenomena accompanying detonations. In the 4th Detonation Symposium in 1967, Hayes reported conductivity measurements in reaction zones in detonation waves in high explosives charges [2]. He ascribed the conductivity to thin graphite sheets formed behind the detonation front. In 1975 and 2000, Ershov also measured ionization during the detonation of TNT cylinders [3, 4]. More recently Kuznetsov et al. have studied the structure of detonation soot in the form of ultra-dispersed diamond and onion carbon [5]. Carbon particles have been observed in the expanding detonation products of LX-10 fireballs (Fig. 1).

In this manuscript we review the subject of carbon particles produced by detonation waves. We consider many facets of the problem, including: (i) Thermodynamic equilibrium solutions, (ii) experimental data such as SEM photographs of the carbon agglomerate structures, (iii) similarity model of conductivity profiles in detonations, (iv) conductivity correlation with carbon content in the explosive, (v) agglomeration kinetics.

THERMODYNAMICS

We consider carbon particles produced by detonation waves in condensed explosives. Table 1 presents the species composition for typical CHNO-based explosives at the Chapman-Jouguet (CJ) state. It shows that the major gaseous species (H₂O, CO₂, N₂, OH⁻, H⁺, CO, NH₃) have similar concentrations at the CJ state. What is unique is the carbon concentration in the condensed state. For example:

- **TNT:** 21.6 moles/kg of carbon graphite
- **Comp B:** 12.7 moles/kg of carbon diamond
- **LX-10:** 7.2 moles/kg carbon diamond
- **Tritonal:** 20.2 moles/kg carbon liquid
- **PETN:** 2.4 moles/kg carbon liquid

Condensed carbon is in fact the dominant species in the detonation products of most CHNO-based explosives.

SEM PHOTOGRAPHY

While thermodynamic codes predict the equilibrium concentrations of the condensed carbon phase, they do not predict the structural form of the carbon. For this one must turn to experiments. Figure 1 shows scanning-electron-microscope (SEM) pictures of Detonation

Nano Diamond (DND) crystals from Comp B. It reveals the densely agglomerated nature of the DND crystals; the typical grain size is $O[5\mu\text{m}]$. The SEM micrograph of Fig. 2 shows graphite ribbons (A) embedded in diamond spheroids (B) for Comp B.

SIMILARITY MODEL

Ershov [3,4] has measured the conductivity profile in a propagating detonation wave in TNT; experimental configuration is shown in Fig. 4. Kuhl [X] has proposed an analytic model of the conductivity profile. It is based on: (i) the similarity solution [7] of the detonation profile, shown in Fig. 5; (ii) condensed carbon concentration from the thermodynamic equilibrium solution of the Cheetah code [6]; and (iii) electron concentration function of Einbinder [10], based on the carbon concentration. Figure 6 shows that this model gives a good mean representation of the measured conductivity profile in a TNT detonation wave.

CORRELATION

Hayes has measured the electrical conductivity in various CHNO explosives. He has shown that the peak conductivity correlates with the carbon concentration in the condensed explosive (see Fig. 7). He fit the data with the following correlation:

$$\log(\sigma_*) = 1.08 + 5.71 * (\varphi_c \rho_0) \quad (1)$$

where

- peak electrical conductivity: $\sigma_* = (\text{mho} / \text{m})$
- carbon content: $C = \varphi_c * \rho_0$
- carbon mass fraction: $\varphi_c = m_c / m_{\text{total}}$
- initial charge density: $\rho_0 = (\text{g} / \text{cc})$

CARBON AGGREGATION KINETICS

Carbon Aggregation Kinetics of Bastea [12] for TATB

$$\frac{DN_b}{Dt} = \alpha N_b + \frac{2}{9} \frac{p_a}{n_0} \frac{k_B T}{\eta} \rho N^{-2} N_n^4 \quad (2)$$

term 1: cluster to fluid; term 2: nuclei to bulk

CONCLUSIONS

Condensed carbon is the most prominent specie in the detonation products of most CHNO explosives. Carbon induces a conductive property to the detonation products; peak conductivity is related to the carbon content of the explosive (Fig. 6). Carbon particulates form one of the major optical emission sources of explosions (Fig. 8). The structure of the condensed carbon takes the form of agglomerates; in one case cited here, the agglomerates contain graphite ribbons with embedded diamond spheroids. Predicting the structural form is beyond the capabilities of existing physics models.

References

1. Cook, M.A., *The Science of High Explosives*, Reinhold Publishing, New York, 1958.
2. Hayes, B. "On the Electrical Conductivity in Detonation Products," *Proc. 4th Symposium on Detonation*, Office of Naval Research, ACR-126, Washington, 595-601, 1967. Also see B. Hayes, "Electrical Measurements in Reaction Zones of High Explosives", *10th Symposium (Int.) on Combustion*, 869-874, 1964.
3. Ershov, A.P., "Ionization during the Detonation of Solid Explosives" *Fizika Gorenija i Vzryva* **11** (6), 938-945, 1974.
4. Ershov, A.P., Satonkina, N.P., Dibirov, O.A., Tsykin, S.V., Yaniklkin, Yu. V., "A Study of the Interaction between Components of Heterogeneous Explosives by the Electrical-Conductivity Method", *Combustion Explosion Shock Waves*, **36** (5), 639-649, 2000.
5. Kuznetsov, V.L, Chuvilin, A.L., Moroz, E. M., Kolomichuk, V.N., Shaikhutdinov, Sh.K. and Butenko, Yu.V., "Effect of Explosion Conditions on the Structure of Detonation Soots: Ultra-disperse Diamond and Onion Carbon", *Carbon* **32** (5), 873-882, 1994.
6. Fried, L. F. CHEETAH 1.22 User's Manual, Report No. **UCRL-MA-117541**, LLNL, 1995.
7. Kuhl, A. L., "On the Structure of Self-Similar Detonation Waves in TNT Charges," *Combustion, Explosion & Shock Waves*, 2015, **51** (1), pp. 72-79.
8. Boronin, A.P., Kapinos, N.V., Krenev, S.A., Mineev, V.N., "Physical Mechanism of Electromagnetic Field Generation during the Explosion of Condensed-explosive Charges: Survey of Literature", *Combustion, Explosion & Shock Waves* **26** (5), 597-602, 1990.
9. Kuhl, A. L, White, D. A., Kirkendall, B., " Electromagnetic Waves from TNT Explosions", *J. Electromagnetic Analysis and Applications* 2014, **6**, pp. 280-295.
10. Einbinder, H. "Generalized Equations for the Ionization of Solid Particles", *J. Chemical Physics* **26** (4), 948–953, 1957.
11. Smith, F.T., "On the Ionization of Solid Particles", *J. Chemical Physics* **28** (4), 746–747, 1958.
12. S. Bastea, "Aggregation kinetics of detonation nanocarbon", *Applied Physics Letters* **100**, 214106, 2012
13. Kuhl et al, "Model of conductivity profiles in TNT detonations", *15th Int. Detonation Symposium*, 2015.

Table 1. Species Composition at the CJ State for Various Explosives*

Species	TNT mol/kg	Comp B mol/kg	LX-10 mol/kg	NM mol/kg	AP-NM mol/kg	TRITONAL mol/kg	PETN mol/kg
—							
H2O	8.04	8.061	6.695		16.7	4.85	
CO2	7.491	7.045	6.813		6.702	1.146	
N2	6.286	10.29	12.63		5.301	4.773	
OH-	1.798	3.645	5.144		1.199	0.8374	
H+	1.798	3.645	6.511		4.076	0.8374	
CO	1.576	0.9256	1.906		0.0152	2.05	
NH3	0.632	0.7089	0.3924		0.000394	1.018	
CH4	6.69E-02	2.24E-02	1.11E-03		0	0.461	
H2	2.10E-02	6.92E-03	3.26E-04		0.000466	0.164	
C2H4	1.37E-02	3.39E-03	—		0	0.176	
C graphite	21.6	0	0	1.593	0	0.231	0
C diamond	0	12.7	7.162	0	0	0	0
C liquid	0	0		0	0	20.2	2.385
Al2O3	0	0		0	0	3.71	0

* thermodynamic equilibrium solution as computed by the Cheetah code [6].

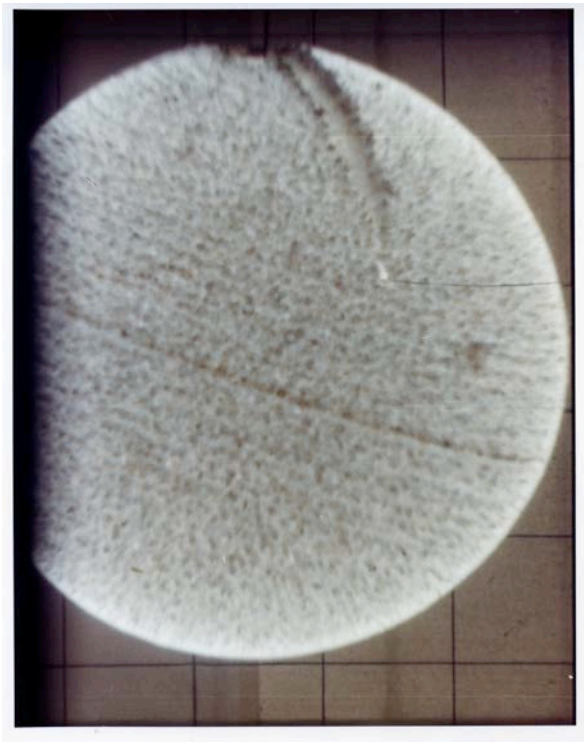


Figure 1. Photograph of the detonation products at $49 \mu s$ after the detonation of an 8-lb sphere of LX-10 (courtesy of F. Sauer, 1981).

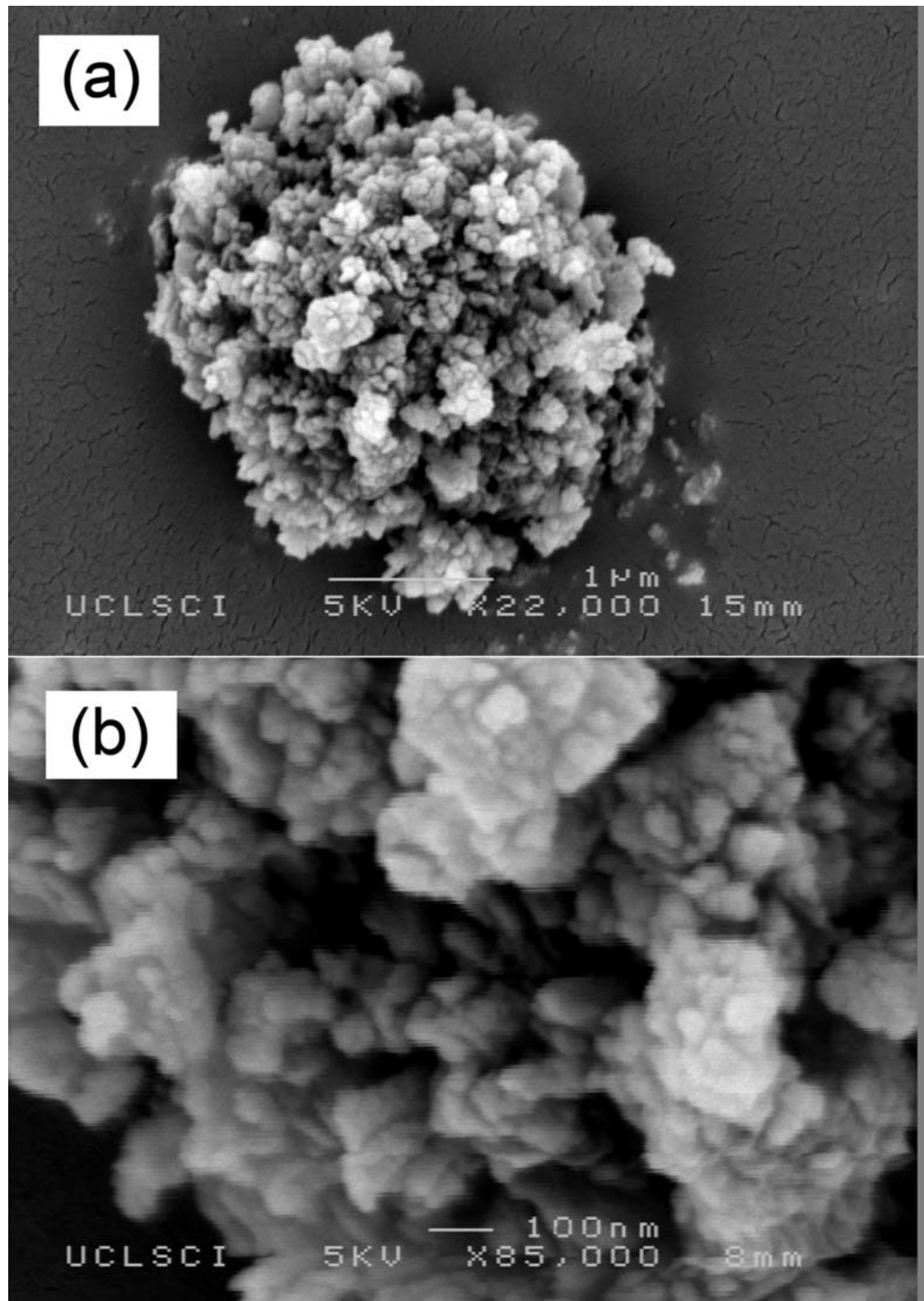


Figure 2. Scanning electron microscope pictures of the DND used revealing (a) typical grain size and (b) the densely agglomerated nature of the DND crystals from Comp B charge (Bevilacqua et al., 2008).

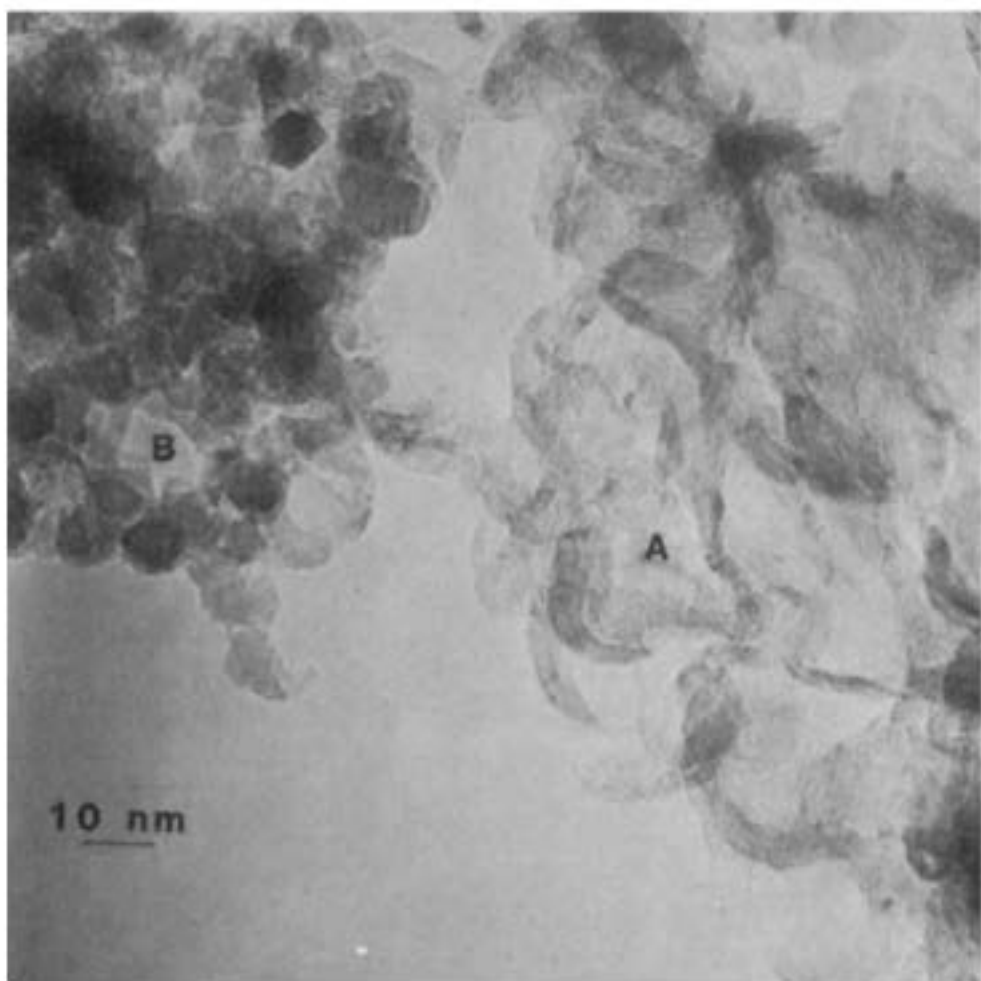


Fig. 1 Electron micrograph of sample 27, scale 10 nm. *A*, Graphite ribbons; *B*, diamond spheroids.

Figure 3. Diamonds in soot from Comp B (Greiner et al., 1988)

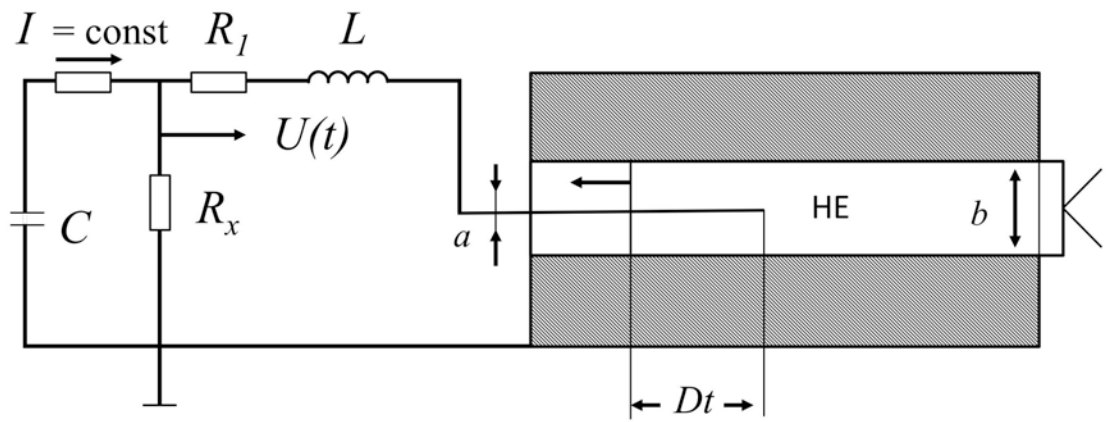


Fig 4. Schematic of the Ershov experiment⁵.

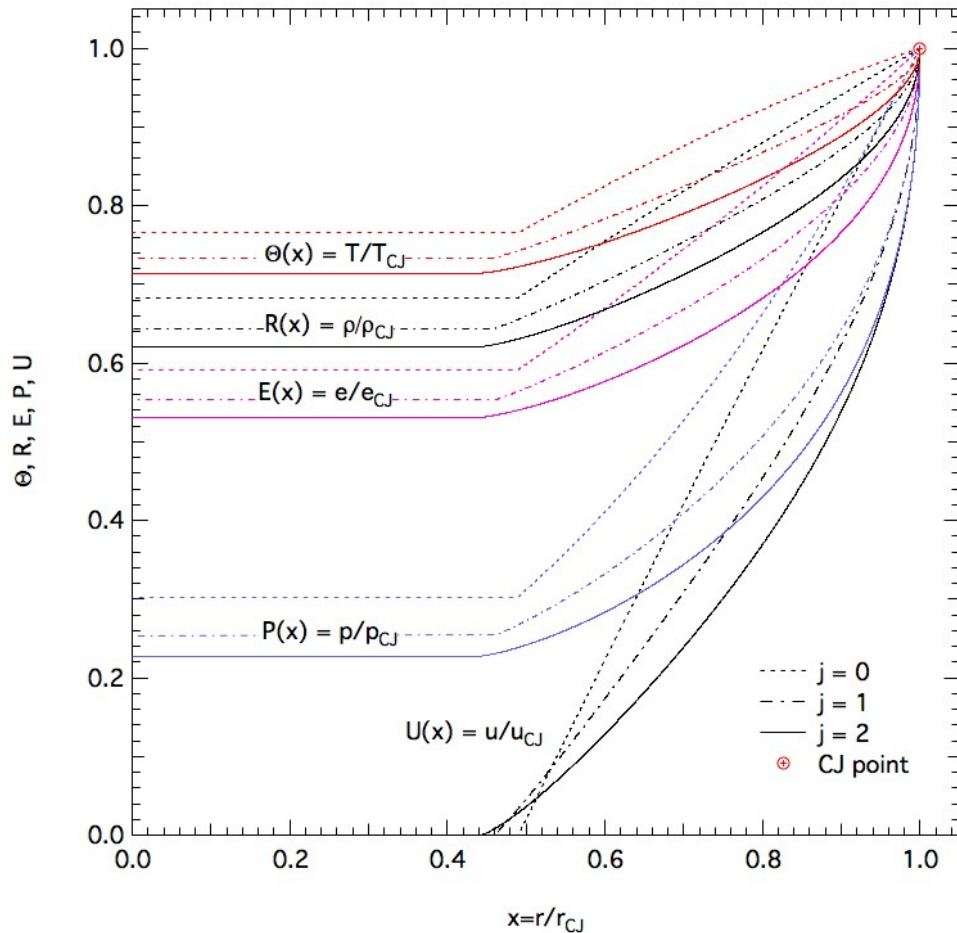


Fig. 5. Similarity solution for planar ($j = 0$), cylindrical ($j = 1$) and spherical ($j = 1$) Chapman-Jouquet detonation waves in TNT by Kuhl⁹.

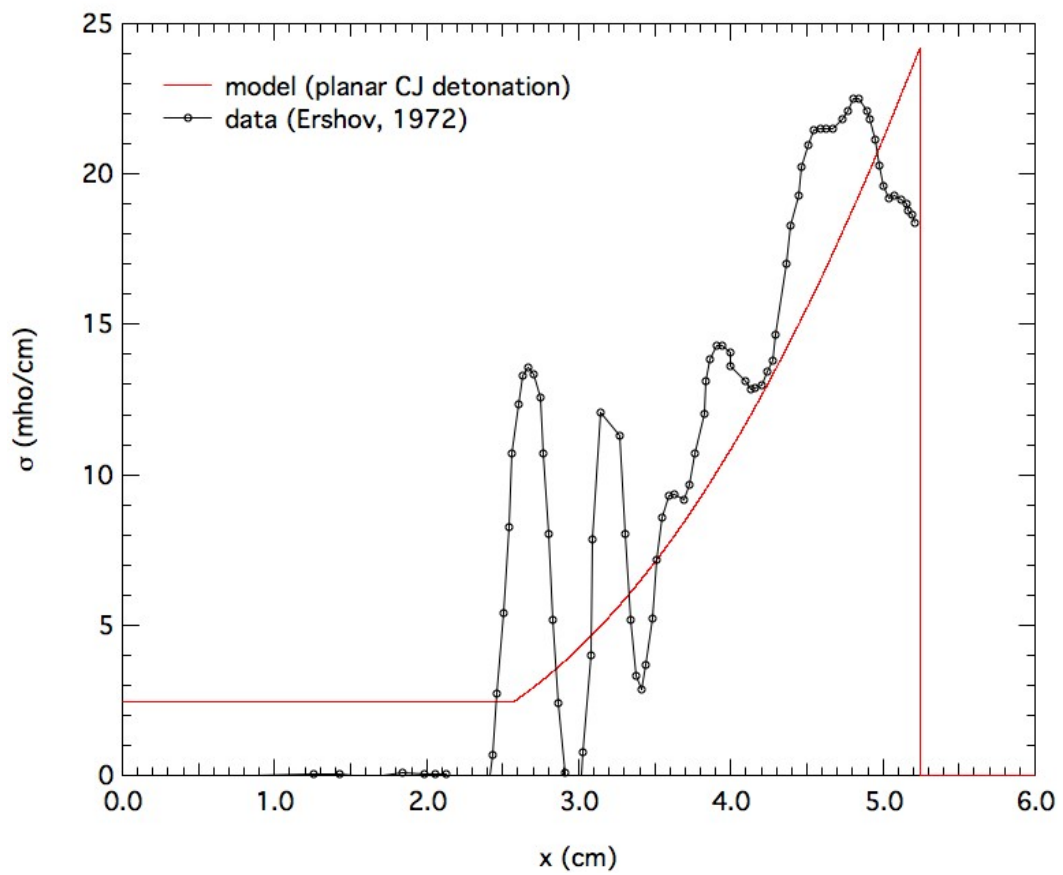


Fig. 6. Conductivity profile in TNT detonation products at $t = 2.5$ us.

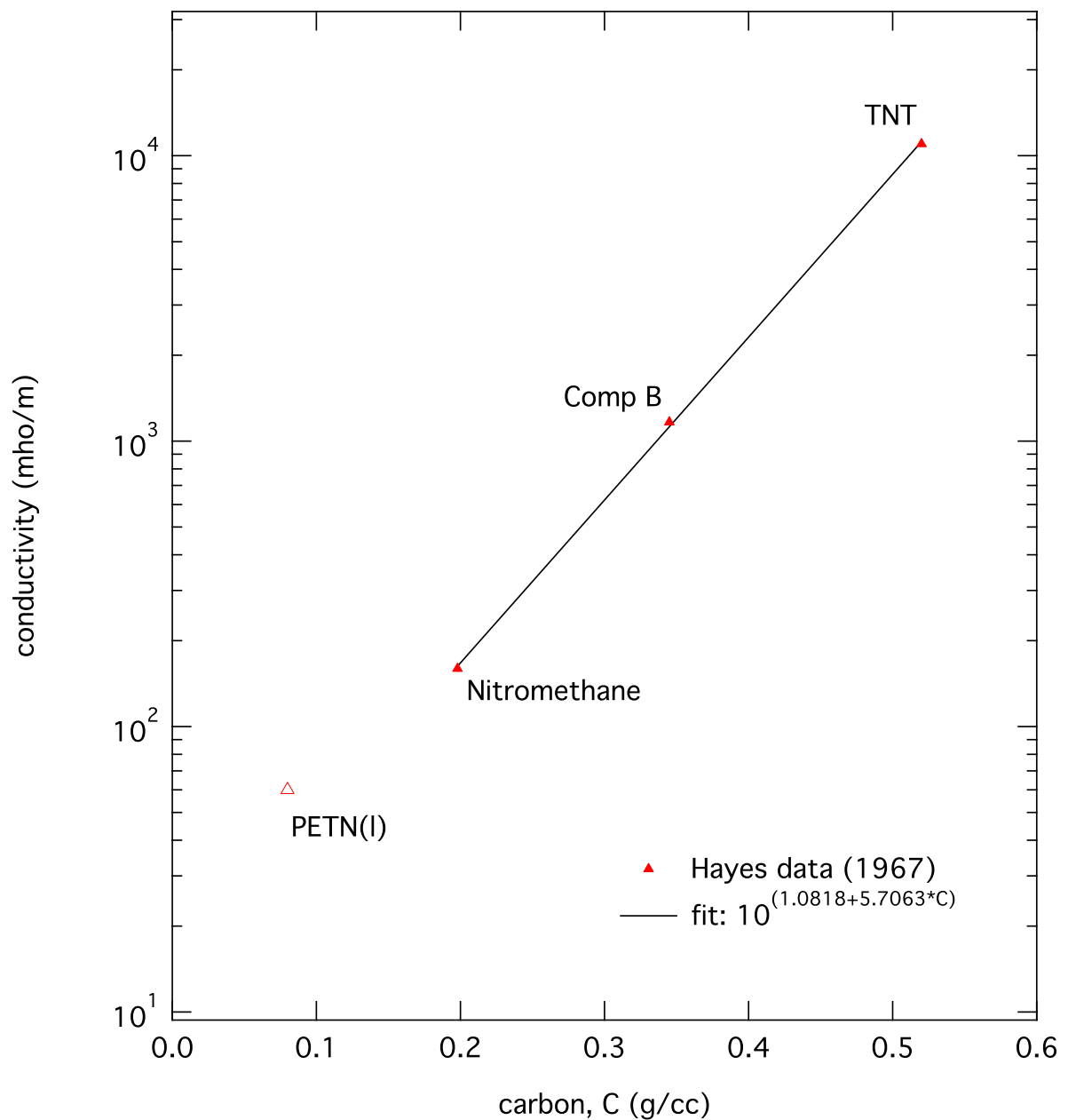


Figure 7. Correlation of peak electrical conductivity with solid-carbon content in the detonation products of various explosives (Hayes, 1967).

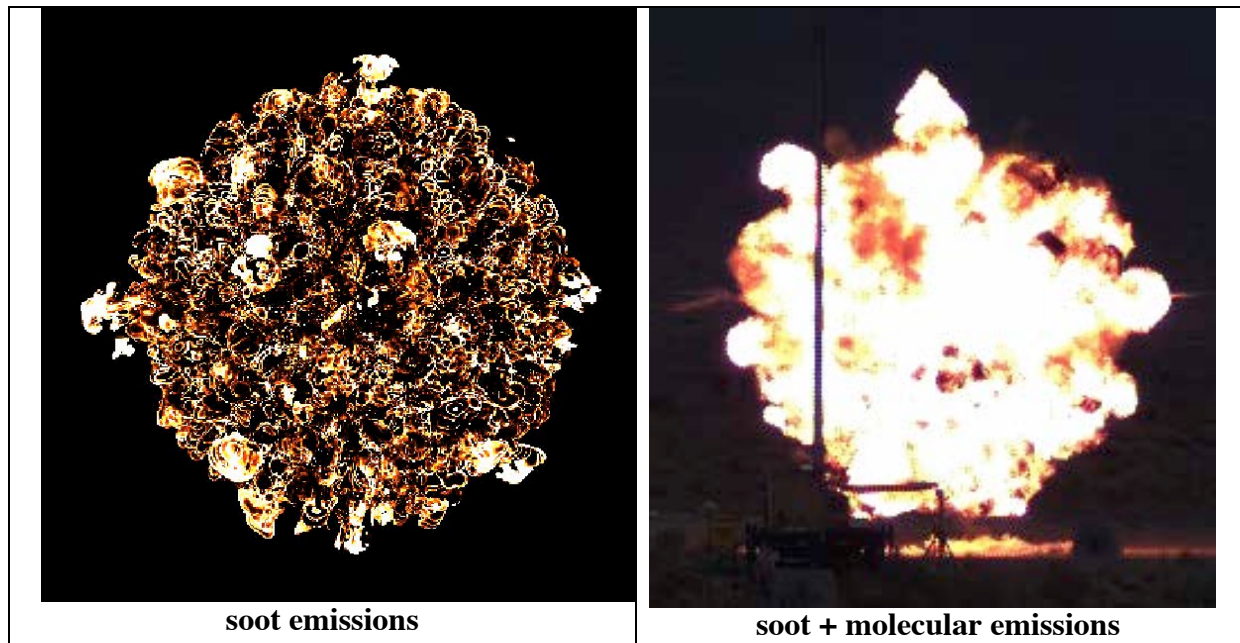


Figure 8. The results can be further processed to produce other diagnostics. For example, the data can be integrated over the image to produce a total power as a function of the wavelength.